

Nuclear Stopping at Intermediate Energies - Experiment versus Simulation



A contour plot showing the nuclear stopping cross-section as a function of projectile and target atomic numbers. The plot features several distinct peaks, with the most prominent one in the upper right quadrant, colored in shades of green and yellow. Other smaller peaks are visible in the lower left and center. The plot is overlaid on a white crosshair against a blue background.

Zoran Basrak

In collaboration with

Philippe Eudes, Maja Zorić and François Sébille



Laboratory for Nuclear Physics
Division of Experimental Physics
Ruđer Bošković Institute, Zagreb, Croatia

Workshop on **Fluctuations and temporal evolution in heavy-ion collisions**
May 9 – 10, 2012, Saclay/Paris, France



Outline

- Energy deposition & stopping in central heavy-ion collisions
- Stopping observables R_E , R_p
- INDRA data on symmetric systems
 $70 < A_{\text{sys}} < 400$, $E_{\text{in}} < 100A \text{ MeV}$
- LV simulation of the same reactions
- Conclusions

Simulation study of central collisions of mass symmetric systems below $100A \text{ MeV}$ in a comprehensive investigation of the role of nuclear EOS & residual collisions



Central collisions

- Above the Coulomb barrier an adiabatic system rearrangement with full stopping and full E dissipation; fusion process

$$E_{\text{DISSIP}} = E_{\text{AVAIL}}$$

- Increasing E : incomplete fusion

$$E_{\text{DISSIP}} < E_{\text{AVAIL}}$$

- From about the Fermi energy E_{Fermi} BDC
 $\sigma_{\text{BDC}} > 95 \% \sigma_{\text{REAC}}$ irrespectively of

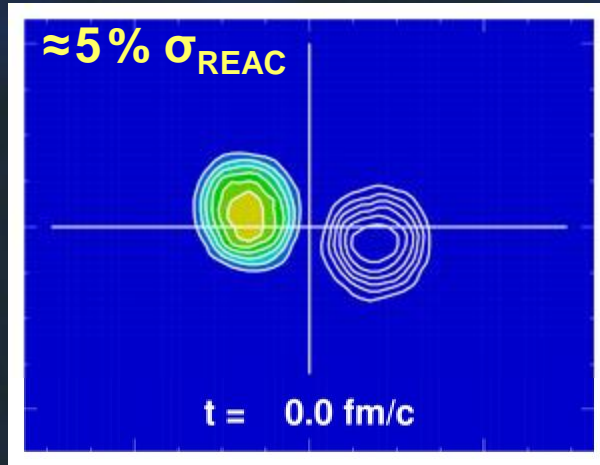
- event centrality
- system size
- system asymmetry

Increasing contribution of hard NN collisions

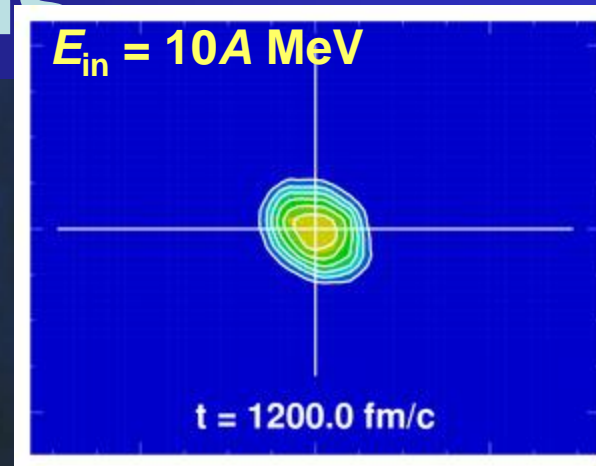


Central collisions

$^{129}\text{Xe} + ^{120}\text{Sn}$



$b = 3 \text{ fm} \approx 0.2 b_{\text{max}}$



$E_x \approx E_{\text{AVAIL}}$
full stopping

Ruđer Bošković

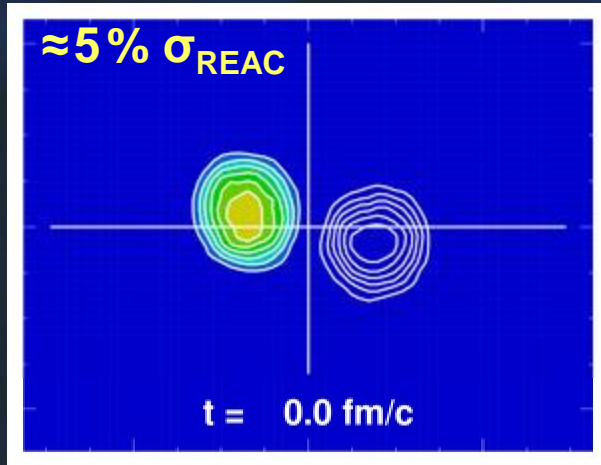


Institute - 1950

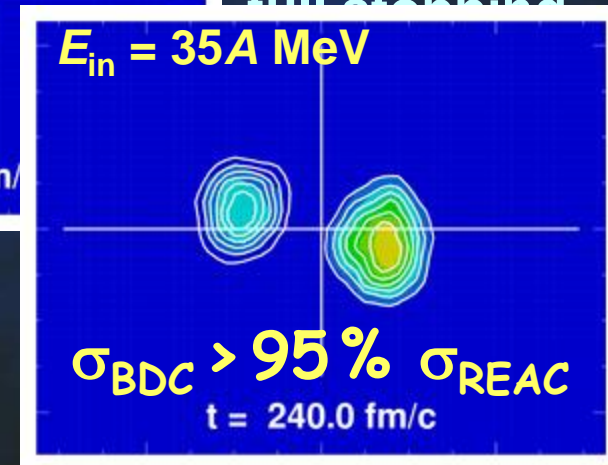
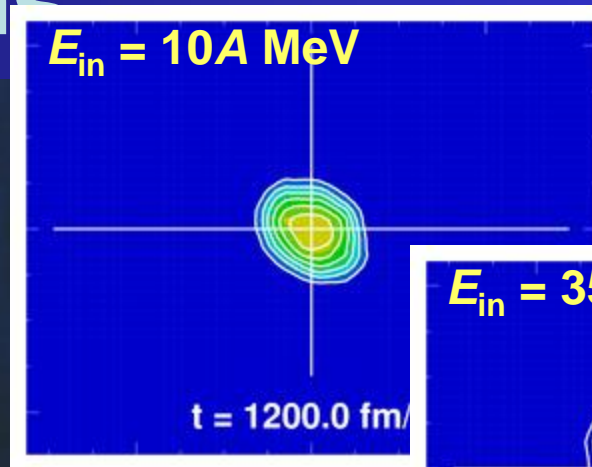
$30 \text{ fm/c} = 1 \cdot 10^{-21} \text{ s}$

Central collisions

$^{129}\text{Xe} + ^{120}\text{Sn}$



$b = 3 \text{ fm} \approx 0.2 b_{\text{max}}$

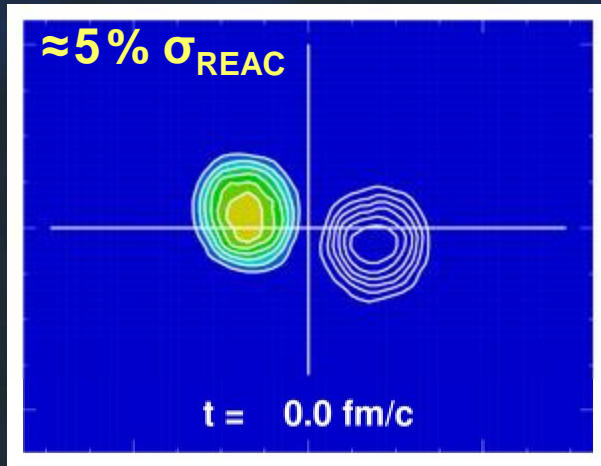


At $E_{\text{Fermi}} (\approx 35A \text{ MeV})$
“hard” NN collisions

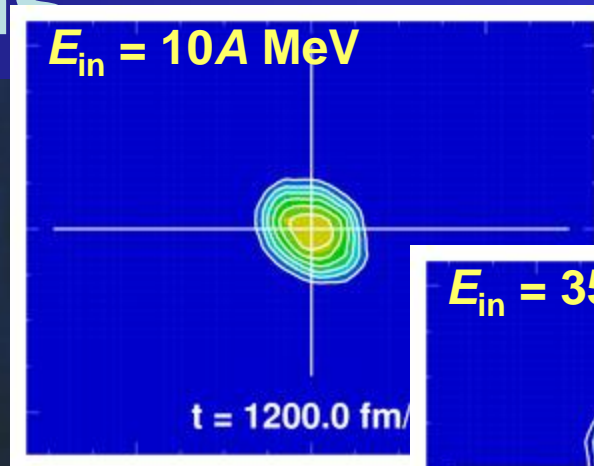


Central collisions

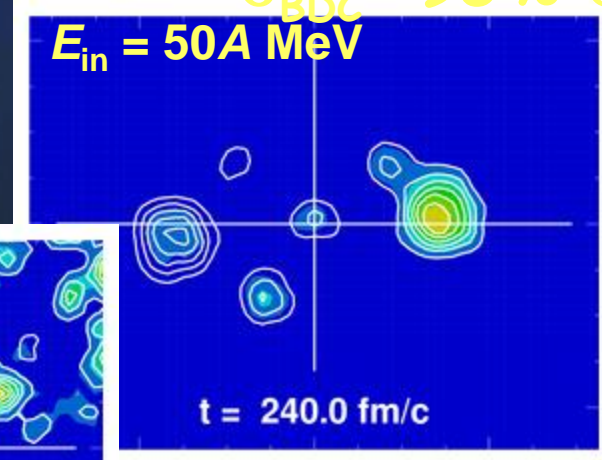
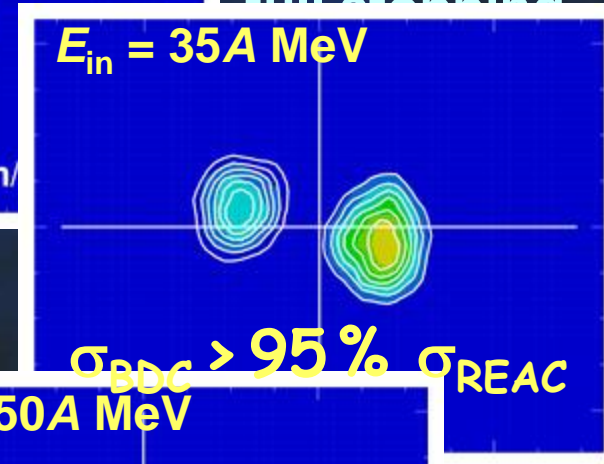
$^{129}\text{Xe} + ^{120}\text{Sn}$



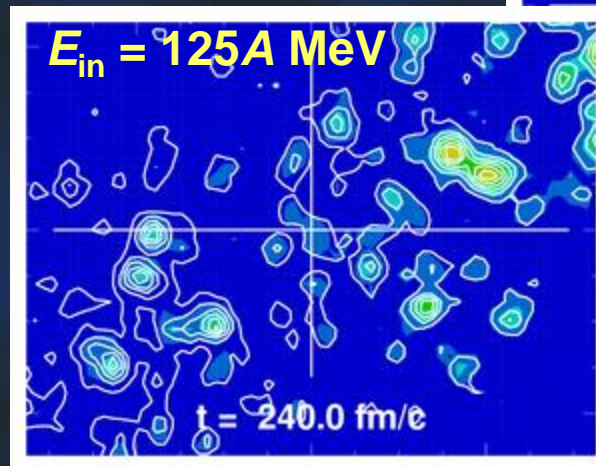
$b = 3 \text{ fm} \approx 0.2 b_{\text{max}}$



$E_x \approx E_{\text{AVAIL}}$
full stopping



(MeV)
sions



$30 \text{ fm/c} = 1 \cdot 10^{-21} \text{ s}$

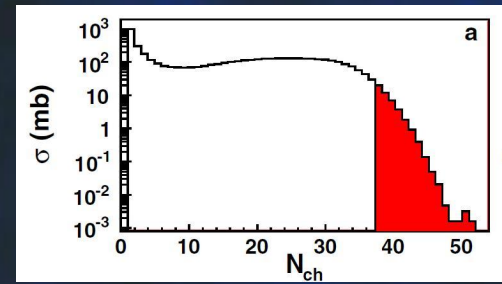


INDRA study of symmetric systems

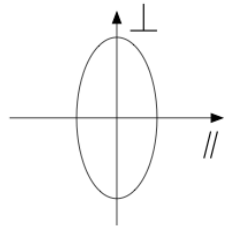
- Ar+KCl, Ni+Ni, Xe+Sn, Au+Au
- Selected ≈ 50 mb (most central)
- Stopping observables R_E (R_p)

$$R_E = \frac{\sum E_{\perp}}{2 \sum E_{\parallel}}$$

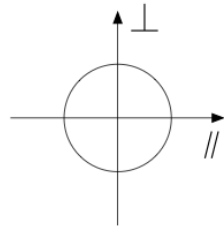
$$R_p = \frac{2 \sum p_{\perp}}{\pi \sum p_{\parallel}}$$



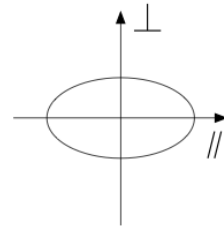
$E_{iso} > 1$



$E_{iso} = 1$



$E_{iso} < 1$



INDRA study of symmetric systems

- Ar+KCl, Ni+Ni, Xe+Sn, Au+Au
- Selected ≈ 50 mb (most central)
- Stopping observables R_E (R_p)

$$R_E = \frac{\sum E_{\perp}}{2 \sum E_{\parallel}}$$

$$R_p = \frac{2 \sum p_{\perp}}{\pi \sum p_{\parallel}}$$

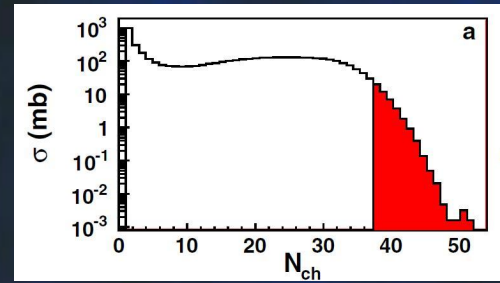
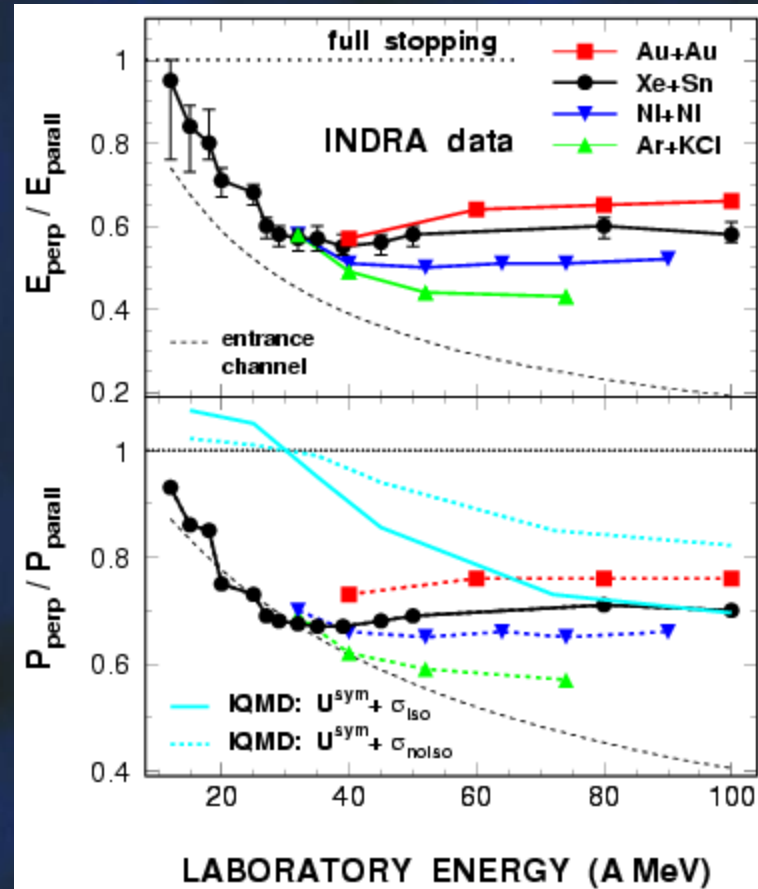


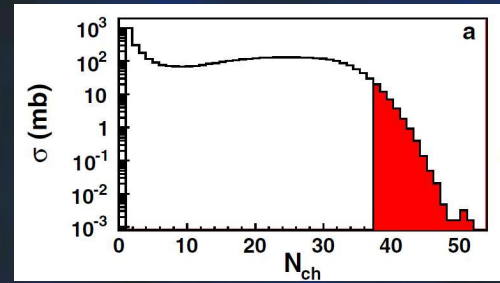
TABLE I. Values of R_E^{central} for different Xe + Sn systems at 32A, 45A, and 100A MeV.

System	N/Z	32 MeV/A	45 MeV/A	100 MeV/A
$^{124}\text{Xe} + ^{112}\text{Sn}$	1.27	0.54	0.53	0.58
$^{129}\text{Xe} + ^{112}\text{Sn}$	1.32	0.60
$^{124}\text{Xe} + ^{124}\text{Sn}$	1.38	0.54	...	0.56
$^{129}\text{Xe} + \text{nat Sn}$	1.38	0.55	0.53	...
$^{136}\text{Xe} + ^{112}\text{Sn}$	1.38	0.50	0.54	...
$^{129}\text{Xe} + ^{124}\text{Sn}$	1.43	0.59
$^{136}\text{Xe} + ^{124}\text{Sn}$	1.5	0.49	0.52	...



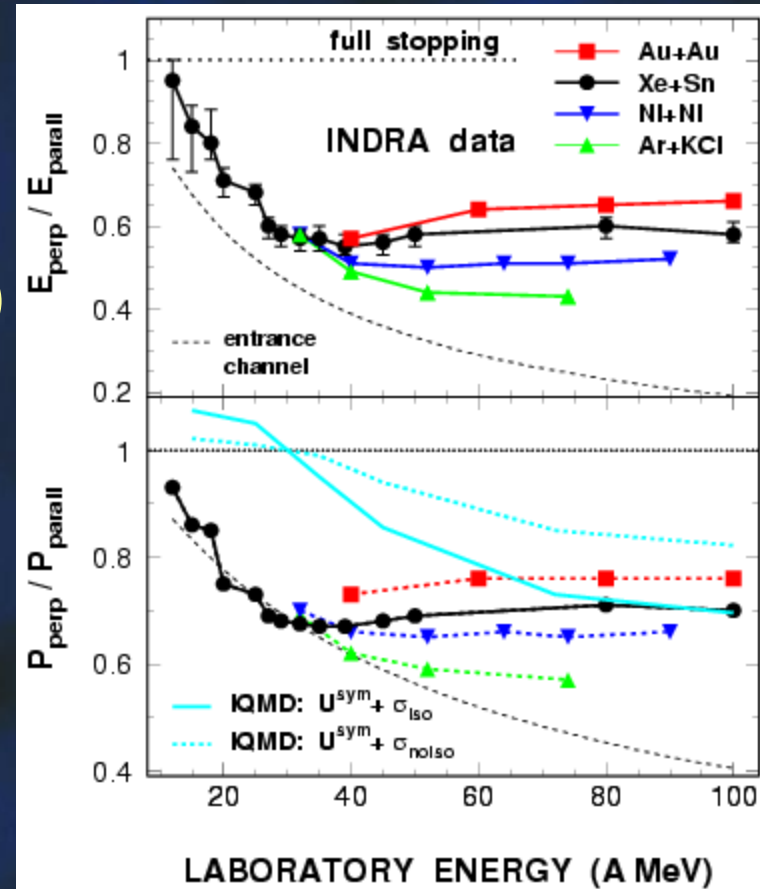
INDRA study of symmetric systems

- Ar+KCl, Ni+Ni, Xe+Sn, Au+Au
- Selected ≈ 50 mb (most central)
- Stopping observables R_E (R_p)



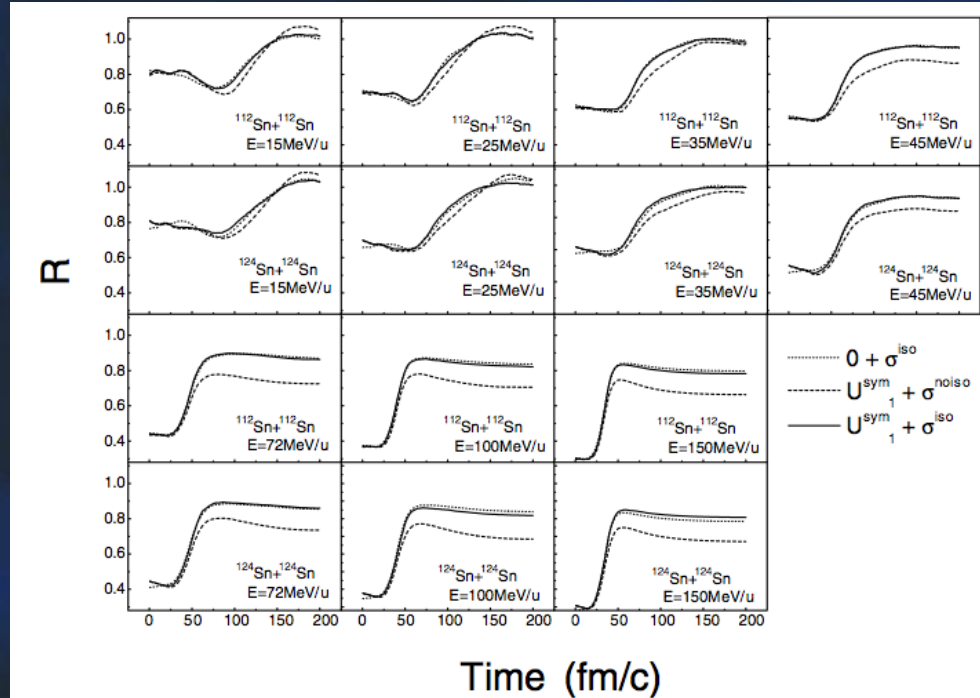
Stopping

- energy dependent (drop followed by constancy)
- transparency ($E_{in} > E_{Fermi}$)
- not isospin dependent



Remadks on IQMD study of R_p

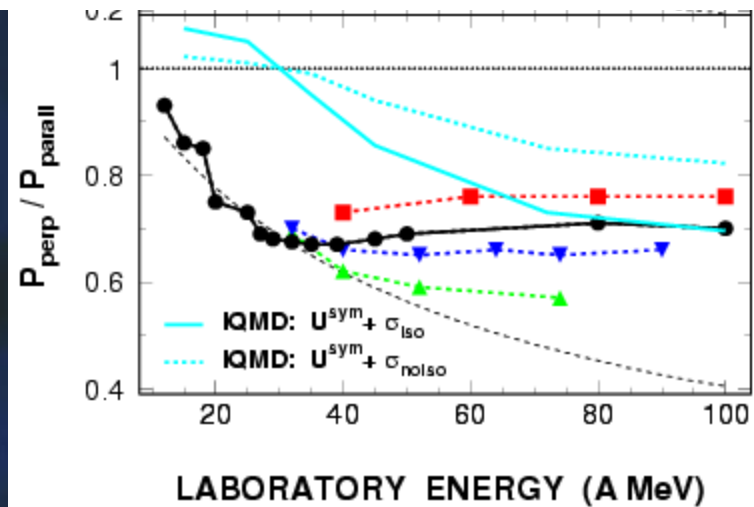
J.-Y. Liu et al., Phys. Rev. Lett. **86** (2001) 975.



$$U = U^{\text{Sky}} + U^{\text{Yuk}} + U^{\text{Coul}} + U^{\text{MDI}} + U^{\text{Pauli}} + U^{\text{Sym}},$$

$$\sigma_{NN}^{\text{med}} = \left(1 + \alpha \frac{\rho}{\rho_0}\right) \sigma_{NN}^{\text{free}}$$

$$\alpha \approx -0.2$$



Ruder Bošković



Institute - 1950

Landau-Vlasov simulation

Transport equation of the Boltzmann type

$$\frac{\partial f}{\partial t} + \{f, H\} = \left(\frac{\partial}{\partial t} + \left(\frac{\mathbf{p}}{m} + \nabla_{\mathbf{p}} U \right) \cdot \nabla_{\mathbf{r}} - \nabla_{\mathbf{r}} U \cdot \nabla_{\mathbf{p}} \right) f = I_{coll}(f)$$

$$H = T + U, \quad U = V_{nucl} + V_{Coul},$$

V_{nucl} : – *Skyrm / Zamick: soft (stiff) local potential*

K=200 (380) MeV, $m^*/m=1.0$ (1.0)

– *Gogny G1-D1 (G3) non-local potentials*

K=228 (360) MeV, $m^*/m=0.67$ (0.68)

$f = f(\mathbf{r}, \mathbf{p}; t)$ - distribution function

Collision term

Phenomenological, (an)isotropic $\sigma = \sigma(E, iso, \theta)$

An approach adequate for bulk (one-body) properties of nuclear dynamics.

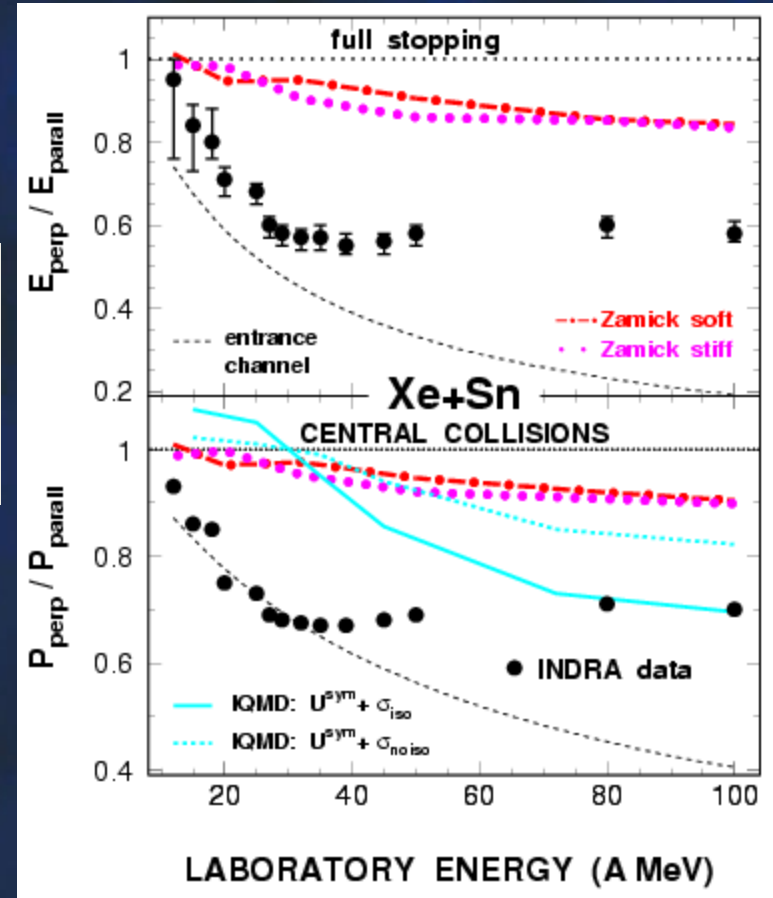


Skyrme/Zamick – local EOS

$$V_{\text{HF}}(\mathbf{r}) = a \frac{\rho(\mathbf{r})}{\rho_0} + b \left[\frac{\rho(\mathbf{r})}{\rho_0} \right]^{1+\nu}$$

TABLE I. Zamick interactions parameters.

Zamick Interaction	a	b	ν	K_∞	m^*/m
Soft	-356	303	1/6	200	1
Stiff	-123	70	1	380	1



Gogny – non-local EOS

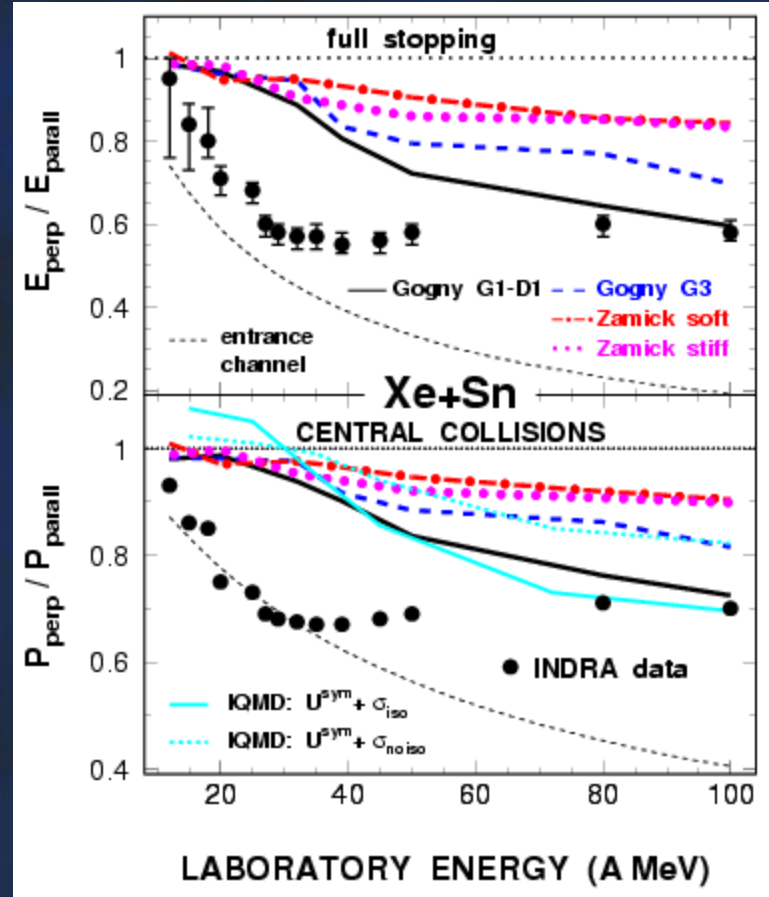
$$V_{\text{HF}}(\mathbf{r}, \mathbf{p}) = \frac{7}{8} t_3 \rho^{4/3}(\mathbf{r}) + \sum_{i=1}^2 \alpha_i \int d^3 r' e^{-(\mathbf{r}-\mathbf{r}')^2/\mu_i^2} \rho(\mathbf{r}') \\ - \sum_{i=1}^2 \beta_i \int d\mathbf{p}' e^{-(\mu_i^2/4\hbar^2)(\mathbf{p}-\mathbf{p}')^2} f(\mathbf{r}, \mathbf{p}'),$$

$$\alpha_i = W_i + \frac{B_i}{2} - \frac{H_i}{2} - \frac{M_i}{4},$$

$$\beta_i = \left[\frac{W_i}{4} + \frac{B_i}{2} - \frac{H_i}{2} - M_i \right] (\sqrt{\pi} \mu_i)^3$$

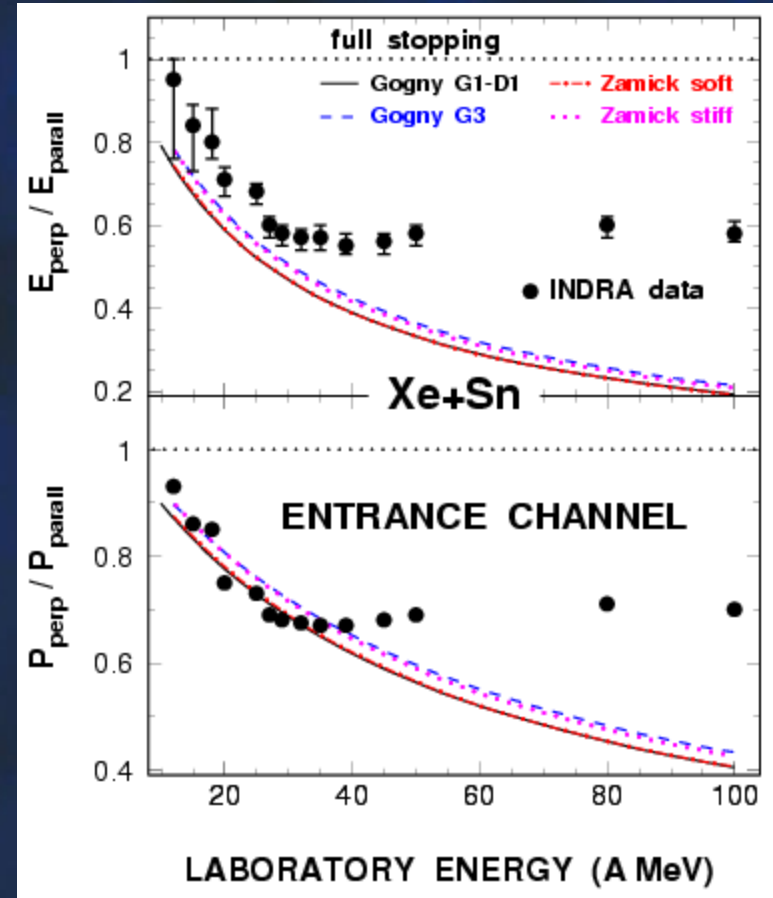
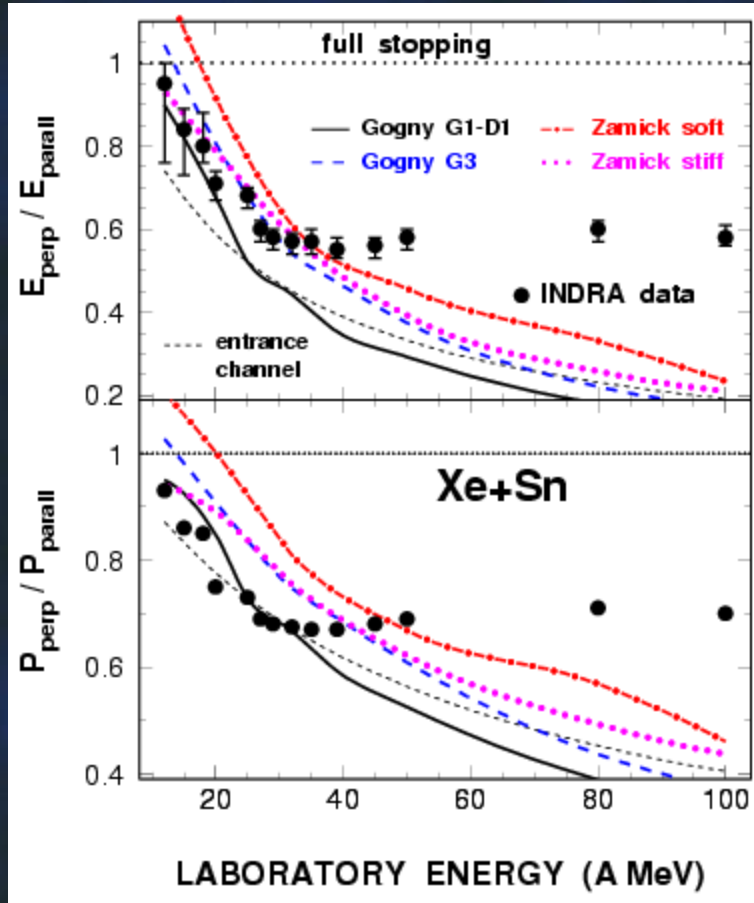
TABLE II. Gogny interaction **G1-D1** parameters.

Gogny Interaction	i	μ_i	W_i	B_i
D1-G1	1	0.7	-402.40	-100.00
	2	1.2	-21.30	-11.77
Gogny Interaction	H_i	M_i	t_3	
D1-G1	-496.20	-22.36	1350	
	-32.27	-68.81	1350	



$$m/m^* = \frac{m}{\hbar^2} \frac{1}{k_F} \left[\frac{d}{dk} \epsilon(k) \right]_{k=k_F} = 0.67$$

Mean field alone (EOS)



At the end of simulation
at $t=240 \text{ fm}/c$

before collision
at $t=0$

NN X section – in medium modifi.

Landau-Vlasov transport equation

$$\frac{\partial f}{\partial t} + \{f, H\} = \left(\frac{\partial}{\partial t} + \left(\frac{\mathbf{p}}{m} + \nabla_{\mathbf{p}} U \right) \cdot \nabla_{\mathbf{r}} - \nabla_{\mathbf{r}} U \cdot \nabla_{\mathbf{p}} \right) f = I_{coll}(f)$$

Collision term

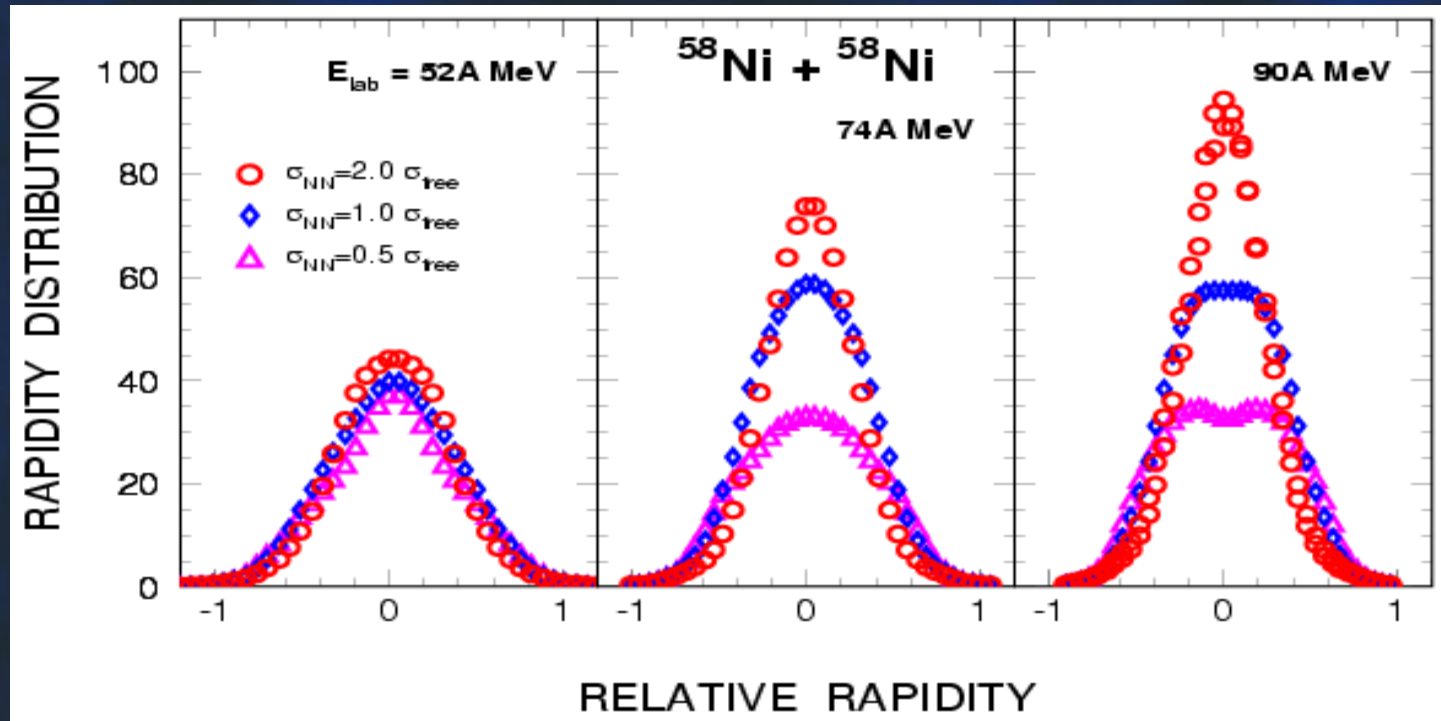
$$(\mathbf{p}, \mathbf{p}_2) \longrightarrow (\mathbf{p}_3, \mathbf{p}_4)$$

$$\begin{aligned} I_{coll} &= I_{coll}^{gain} - I_{coll}^{perte} = \frac{g}{4m^2} \cdot \frac{1}{\pi^3 \hbar^3} \int d\mathbf{p}_2 d\mathbf{p}_3 d\mathbf{p}_4 \frac{d\sigma}{d\Omega} \\ &\times \delta(\mathbf{p} + \mathbf{p}_2 - \mathbf{p}_3 - \mathbf{p}_4) \delta(p^2 + p_2^2 - p_3^2 - p_4^2) \\ &\times [(1 - \bar{f})(1 - \bar{f}_2)f_3f_4 - (1 - \bar{f}_3)(1 - \bar{f}_4)f_2f] \end{aligned}$$

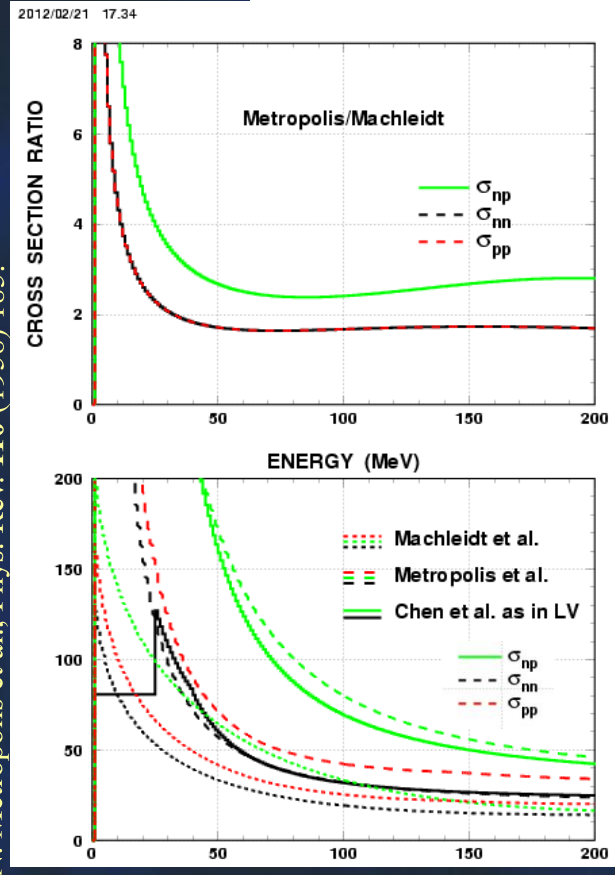
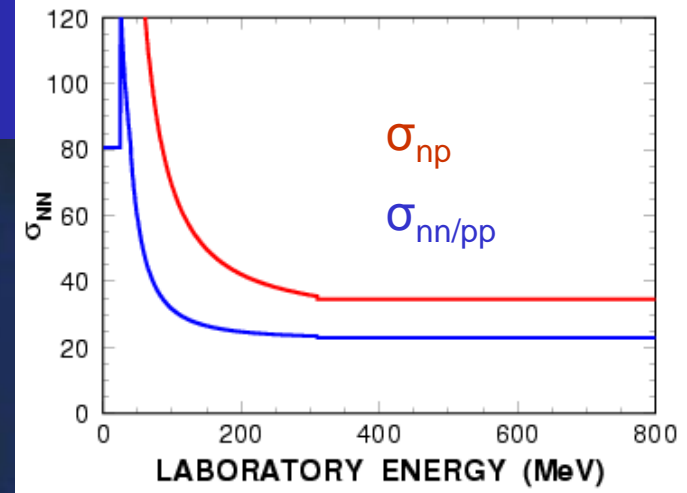
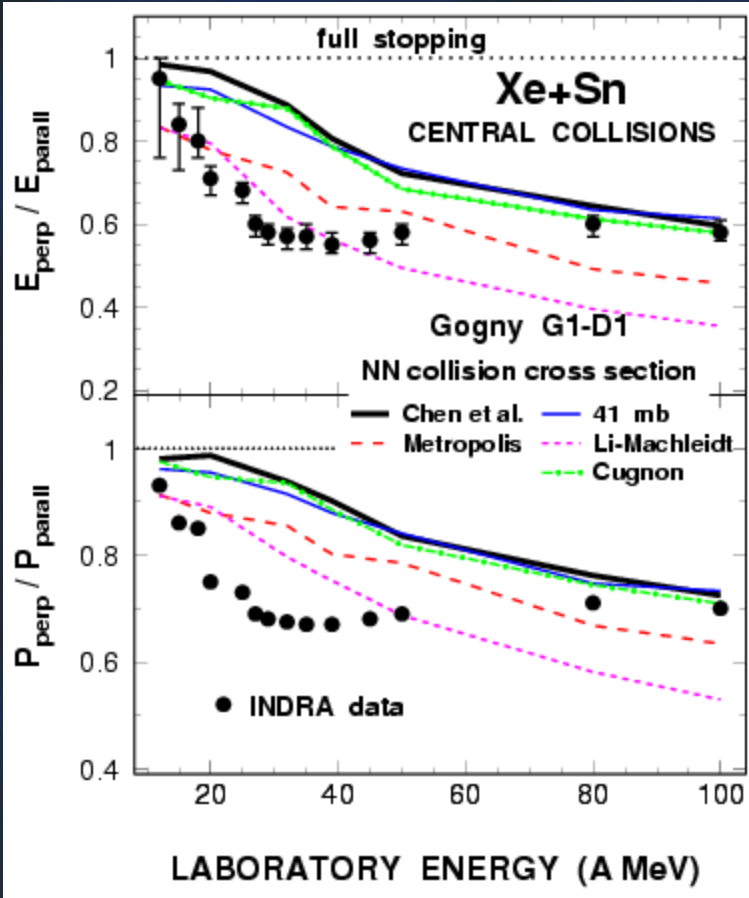


Stopping – rapidity distributions

Besides on nuclear EOS stopping strongly depends on residual nucleon-nucleon cross section σ_{NN}



NN cross section



$\sigma_{\text{Cugnon}} = \sigma_{\text{Chen}} + \text{a weak dependence on density}$

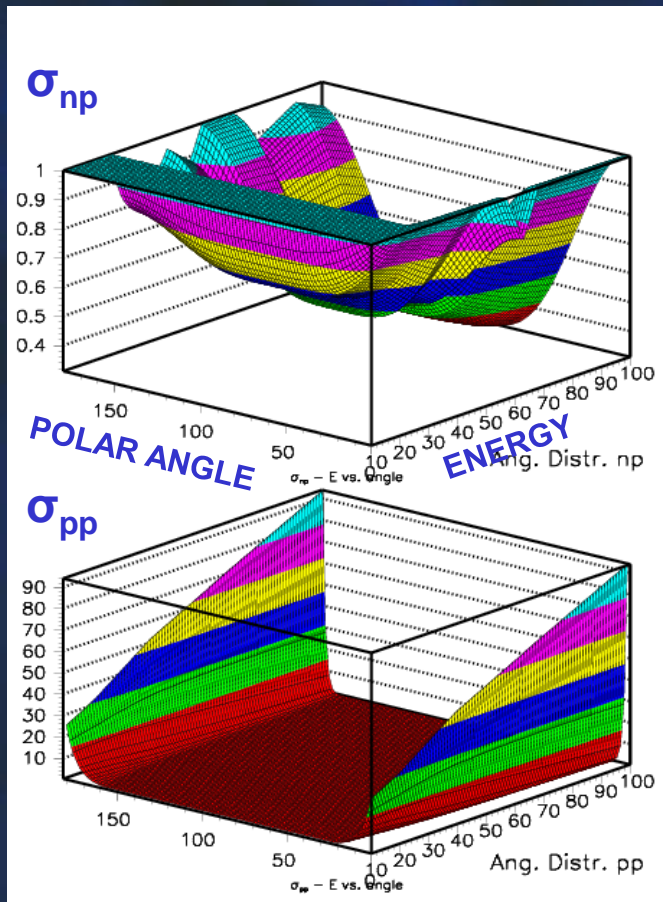
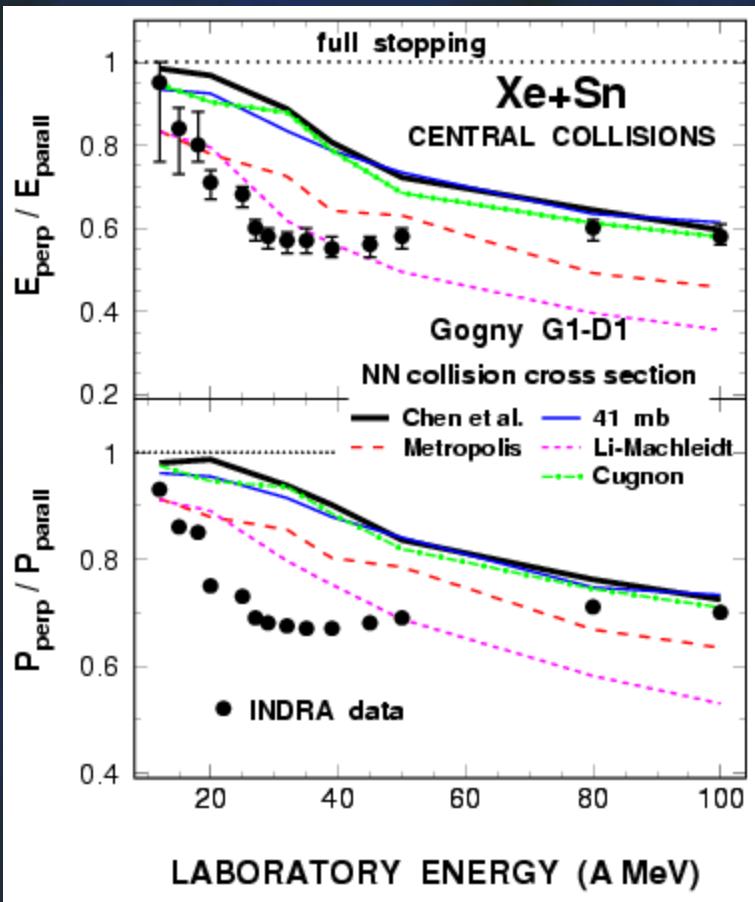
N. Metropolis et al., Phys. Rev. **110** (1958) 185.

G.Q. Li and R. Machleidt, Phys. Rev. **C48** (1993) 1702; **C49** (1994) 1566.

K. Chen et al., Phys. Rev. **166** (1968) 949.



NN cross section



$\sigma_{\text{Li-Machleidt}}$ besides on angle has a strong dependence on density



NN X section – in medium modifict.

Landau-Vlasov transport equation

$$\frac{\partial f}{\partial t} + \{f, H\} = \left(\frac{\partial}{\partial t} + \left(\frac{\mathbf{p}}{m} + \nabla_{\mathbf{p}} U \right) \cdot \nabla_{\mathbf{r}} - \nabla_{\mathbf{r}} U \cdot \nabla_{\mathbf{p}} \right) f = I_{coll}(f)$$

Collision term

$$(\mathbf{p}, \mathbf{p}_2) \longrightarrow (\mathbf{p}_3, \mathbf{p}_4)$$

$$\begin{aligned} I_{coll} &= I_{coll}^{gain} - I_{coll}^{perte} = \frac{g}{4m^2} \cdot \frac{1}{\pi^3 \hbar^3} \int d\mathbf{p}_2 d\mathbf{p}_3 d\mathbf{p}_4 \frac{d\sigma}{d\Omega} \\ &\times \delta(\mathbf{p} + \mathbf{p}_2 - \mathbf{p}_3 - \mathbf{p}_4) \delta(p^2 + p_2^2 - p_3^2 - p_4^2) \\ &\times [(1 - \bar{f})(1 - \bar{f}_2)f_3f_4 - (1 - \bar{f}_3)(1 - \bar{f}_4)f_2f] \end{aligned}$$

$$\frac{d\sigma}{d\Omega} = F \frac{d\sigma_{Chen}}{d\Omega}$$

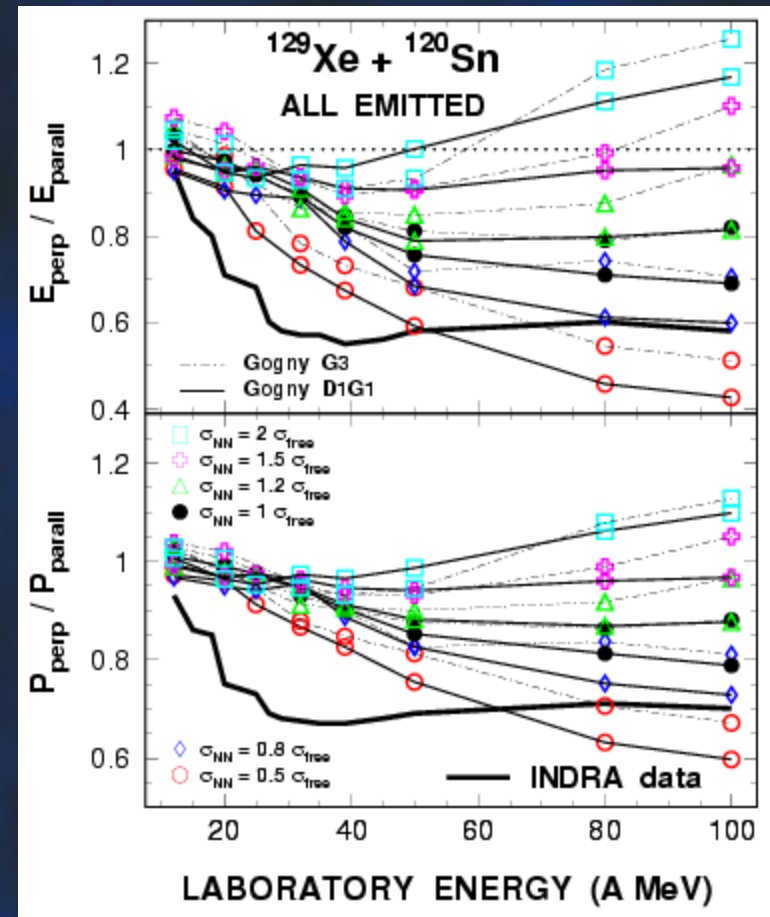
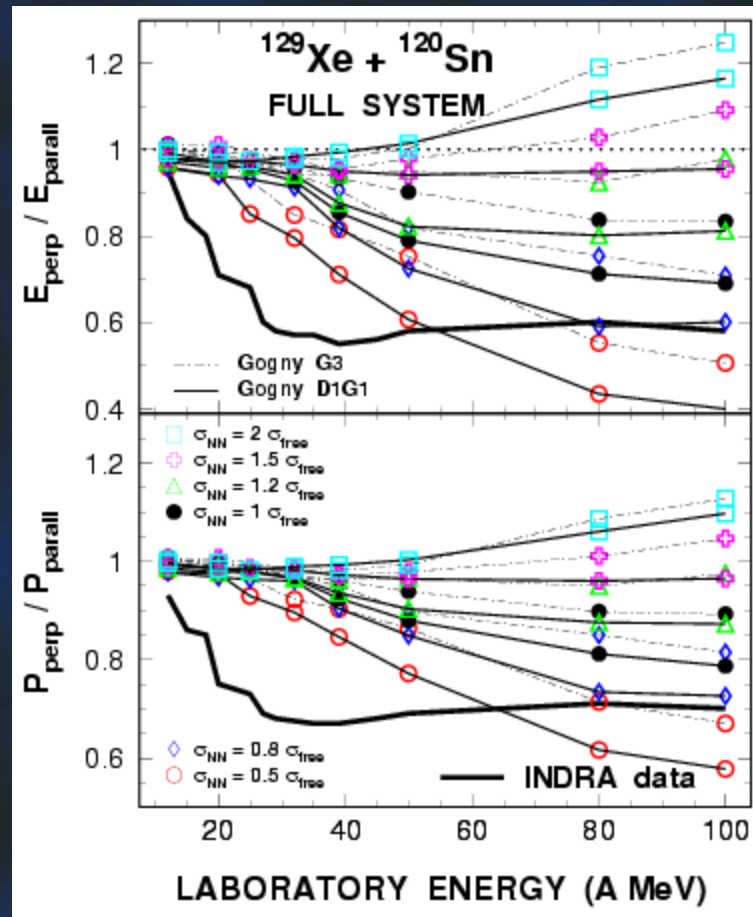
phenomenological $\sigma_{Chen} = \sigma(E, iso)$

$$F = (0.0) 0.5, 0.8, 1, 1.2, 1.5 \text{ and } 2$$



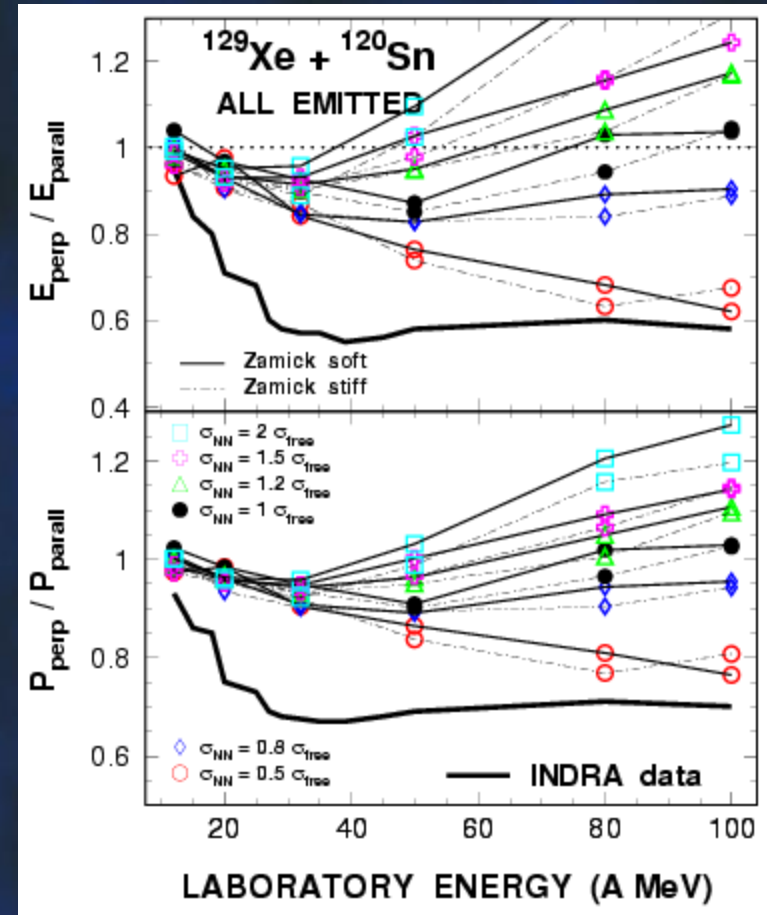
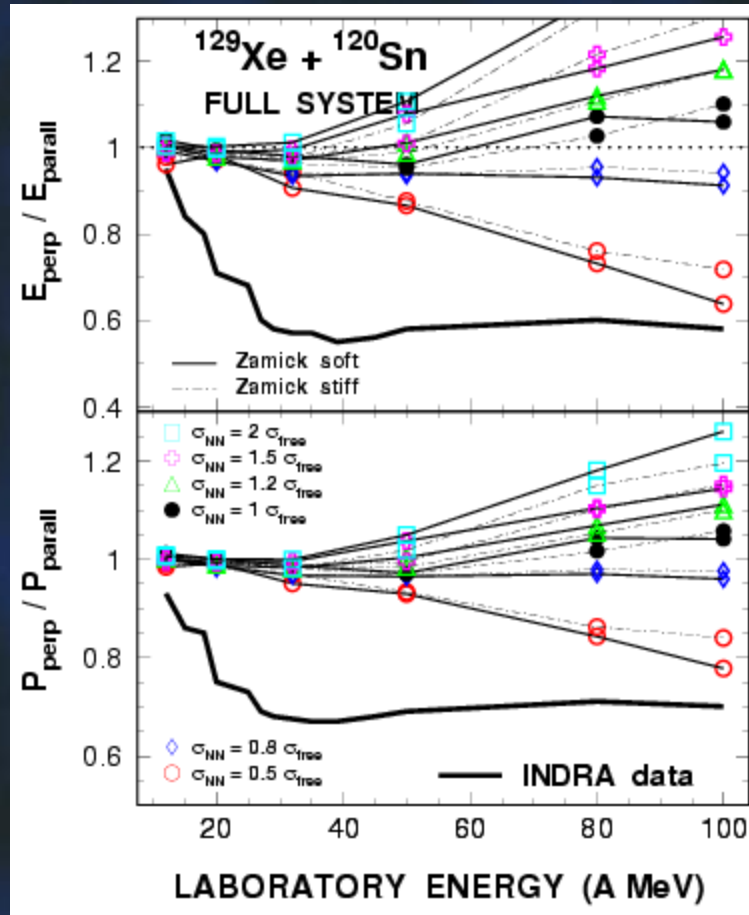
In medium modification

Gogny EOS G1-D1 (soft) and G3 (stiff)

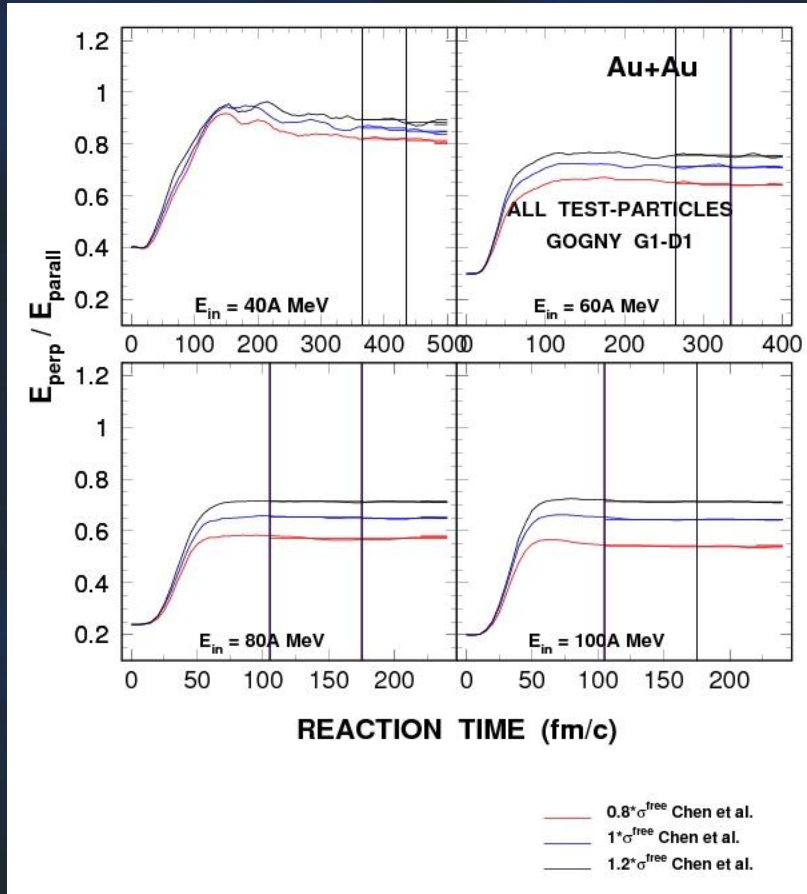


In medium modification

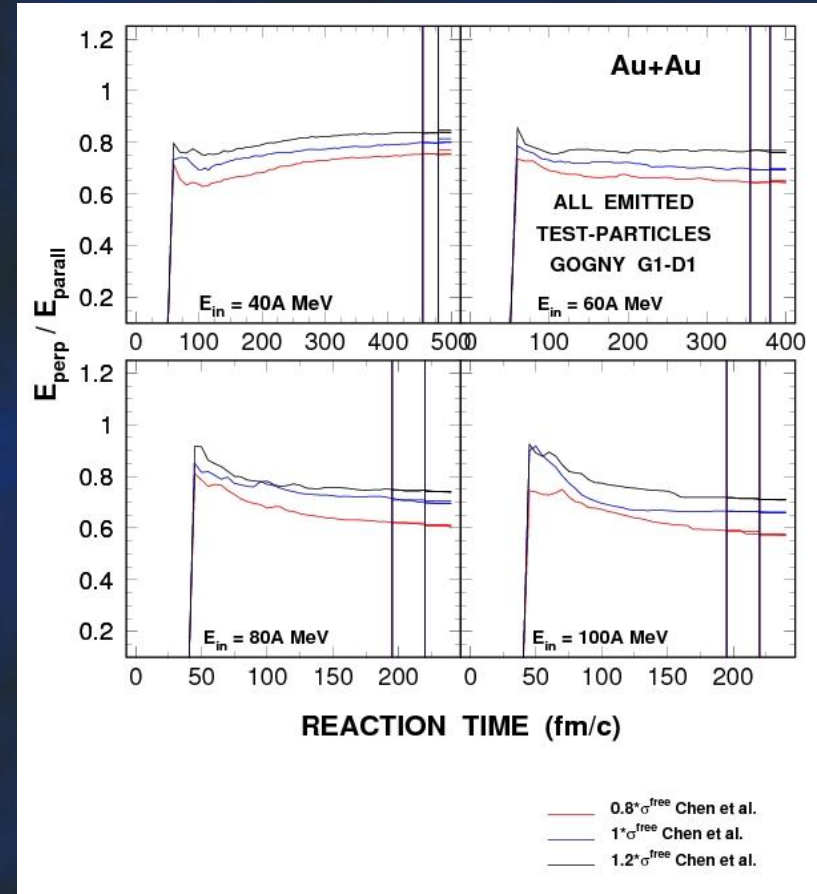
Skyrme / Zamick EOS: soft and stiff



Temporal evolution of R_E



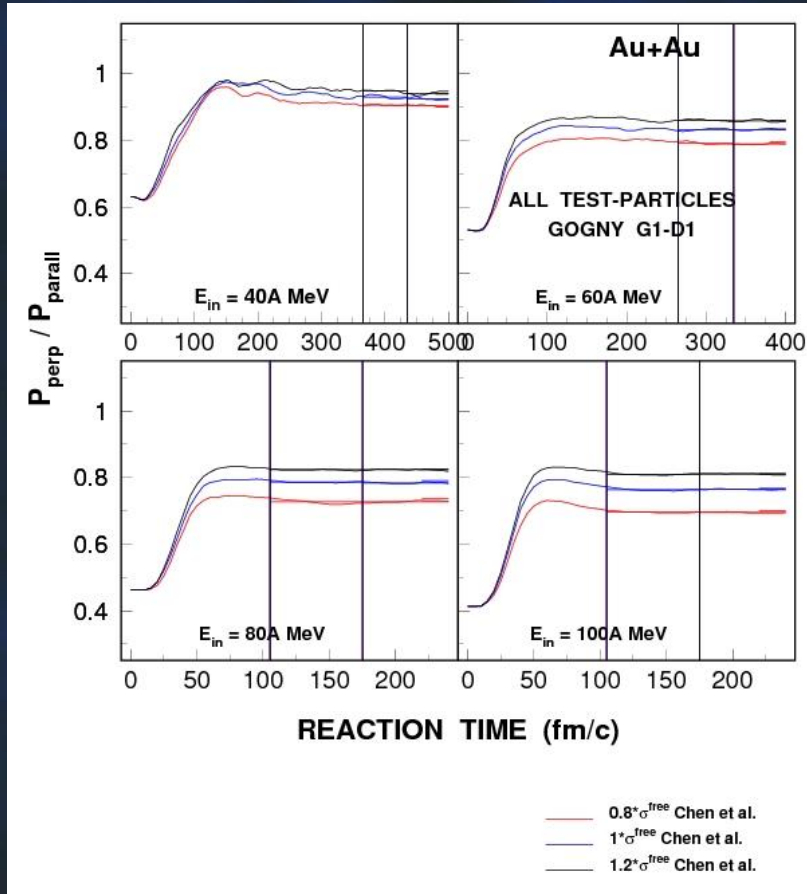
Full system



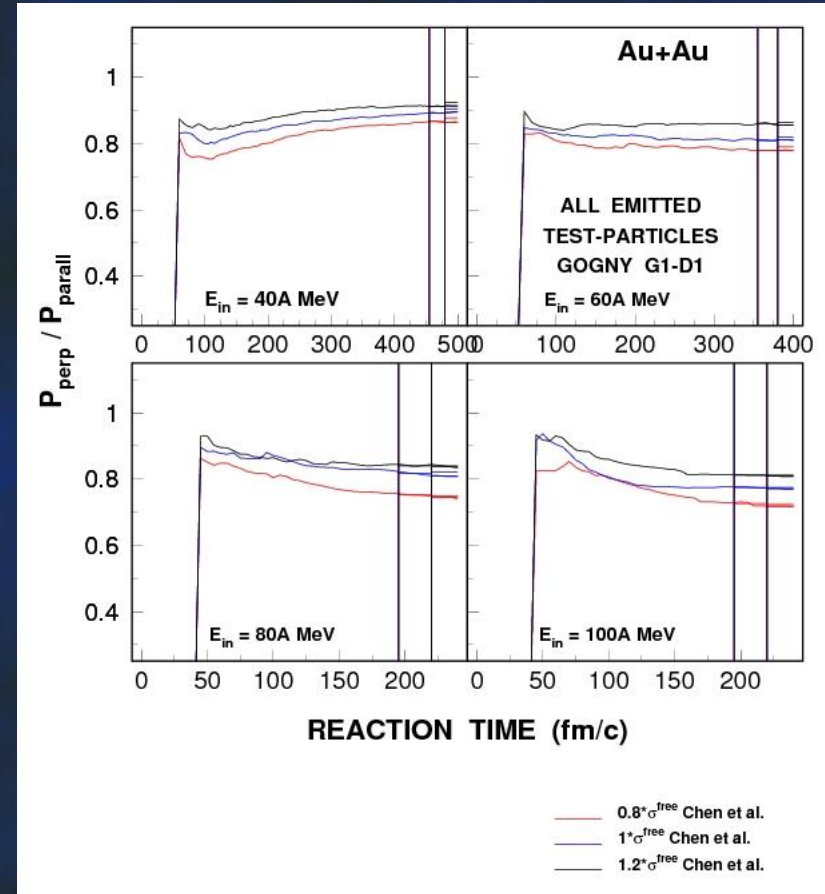
Free (emitted) "particles"



Temporal evolution of R_p



Full system

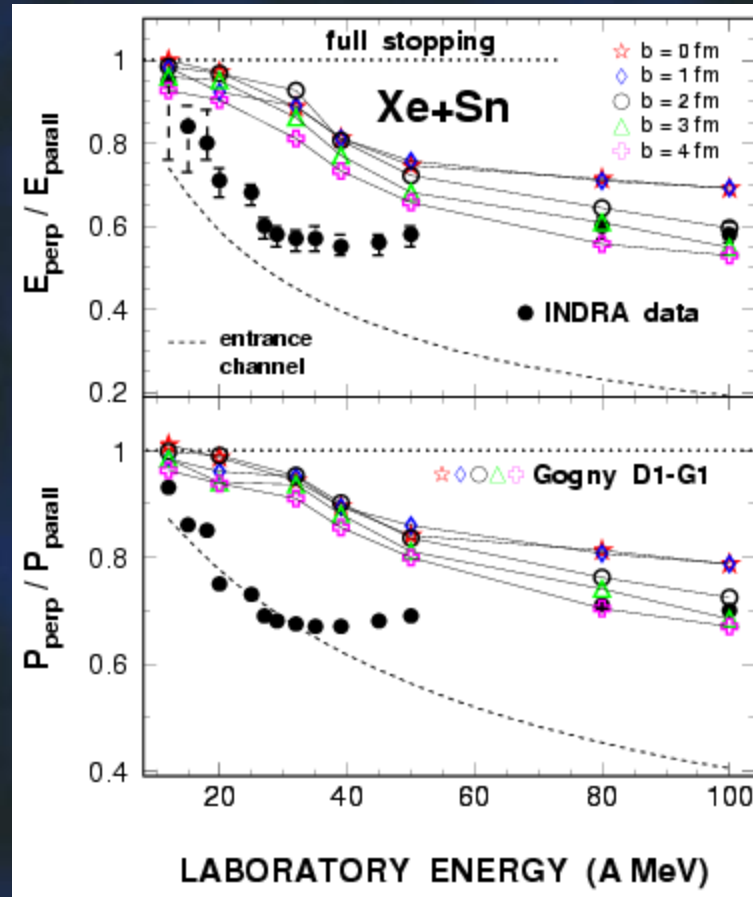


Free (emitted) "particles"

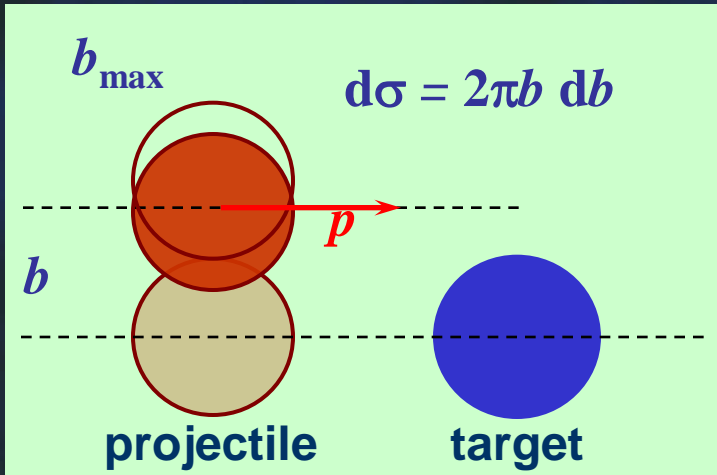


Central collisions & impact param.

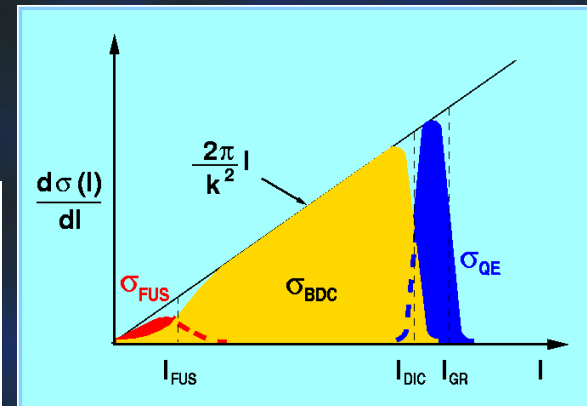
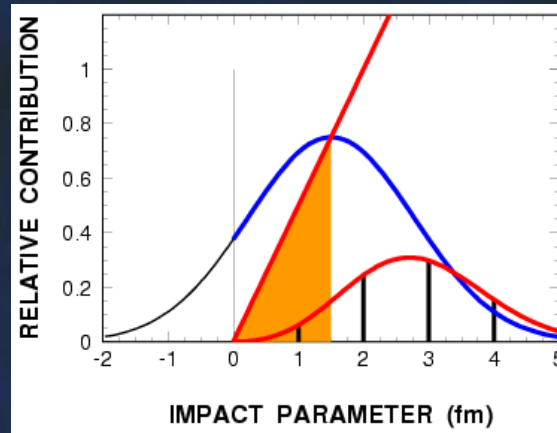
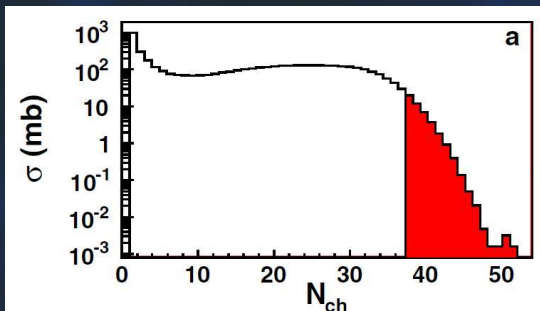
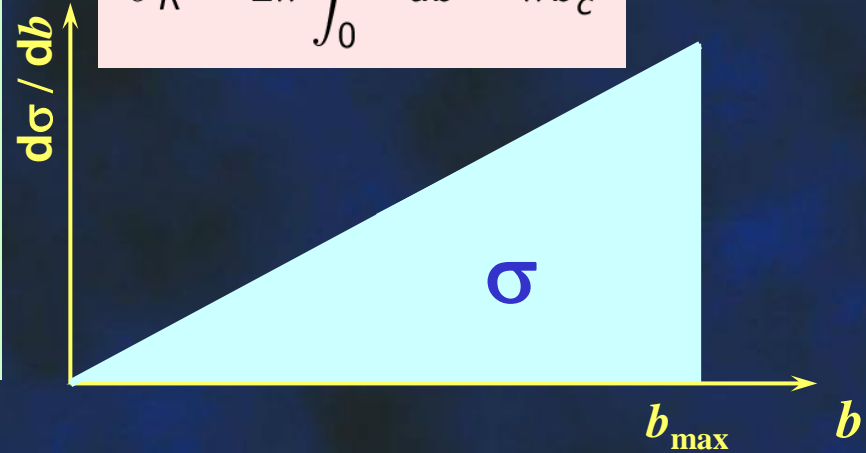
RE , Rp as a function of impact parameter b



Central collisions & impact param.

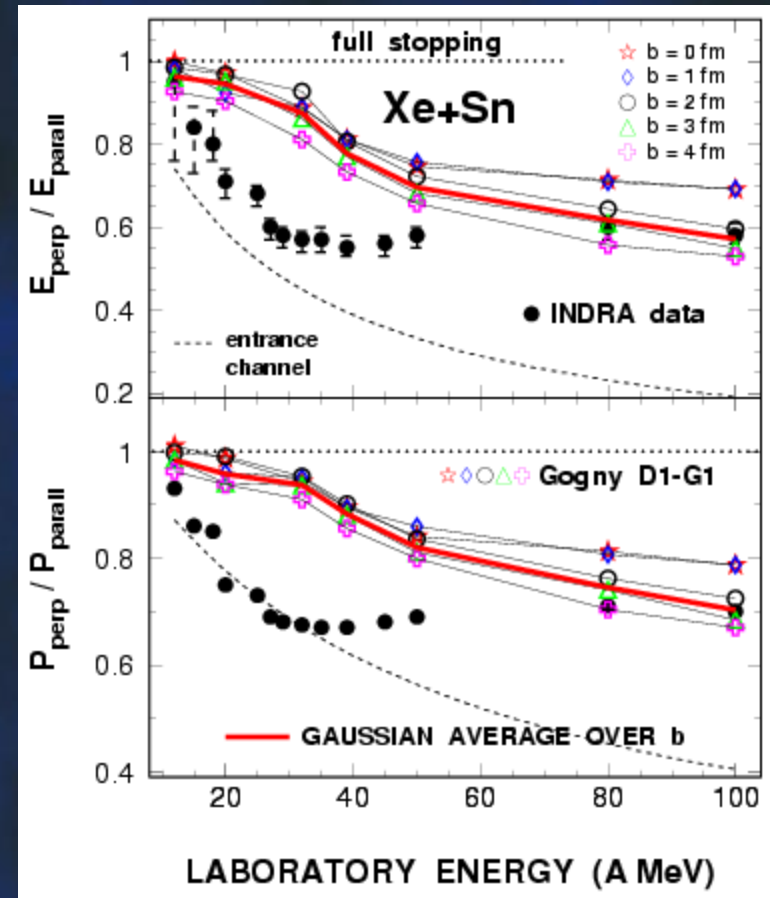
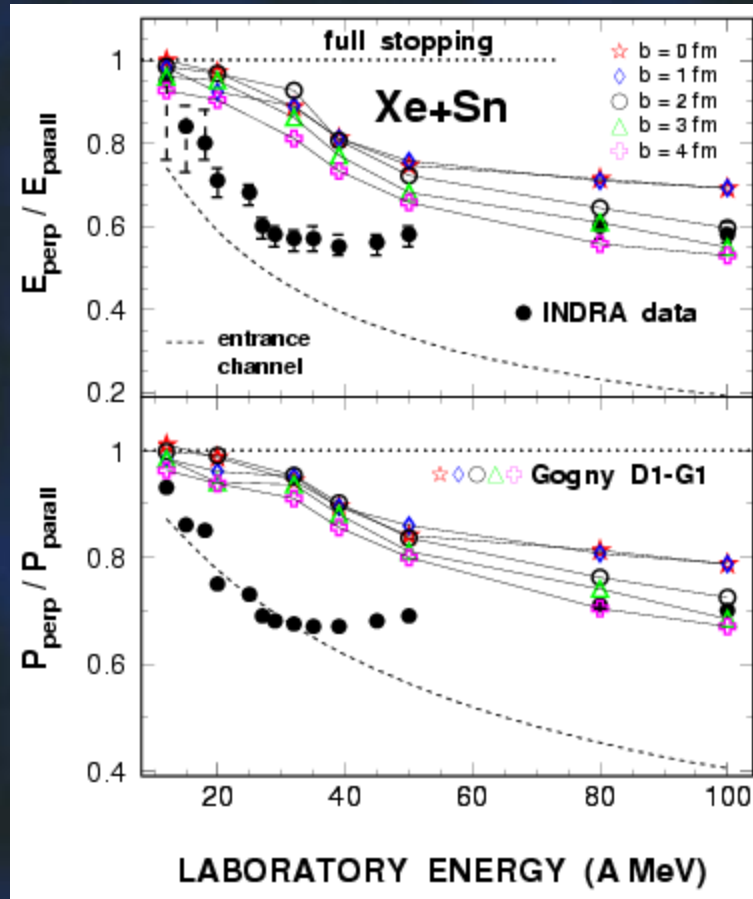


$$\sigma_R = 2\pi \int_0^{b_c} db = \pi b_c^2$$



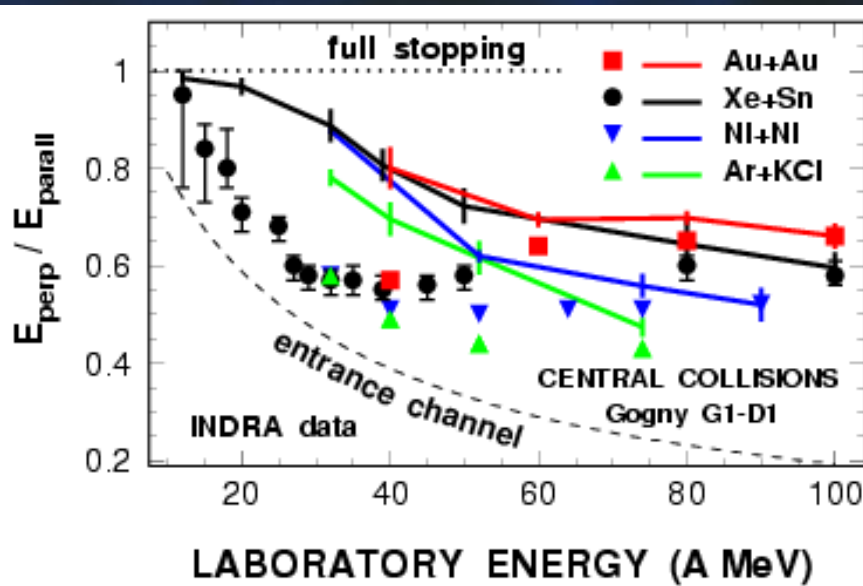
Central collisions & impact param.

RE , Rp as a function of impact parameter b

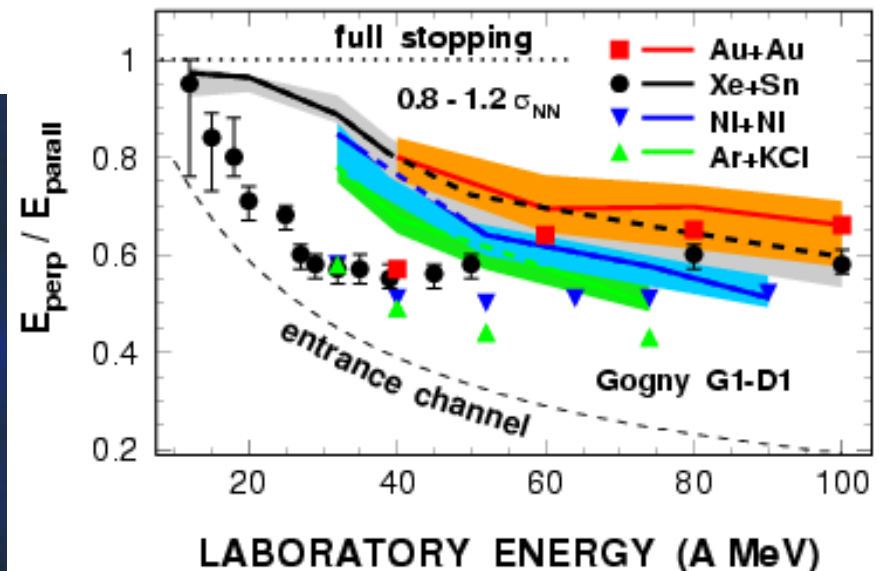


System size

Ar+KCl, Ni+Ni, Xe+Sn, Au+Au



- Correct system mass dependence
- Fails below $E_{lin} \approx 60A$ MeV
- Largest discrepancy around E_{Fermi}
- Correct at low E_{in}

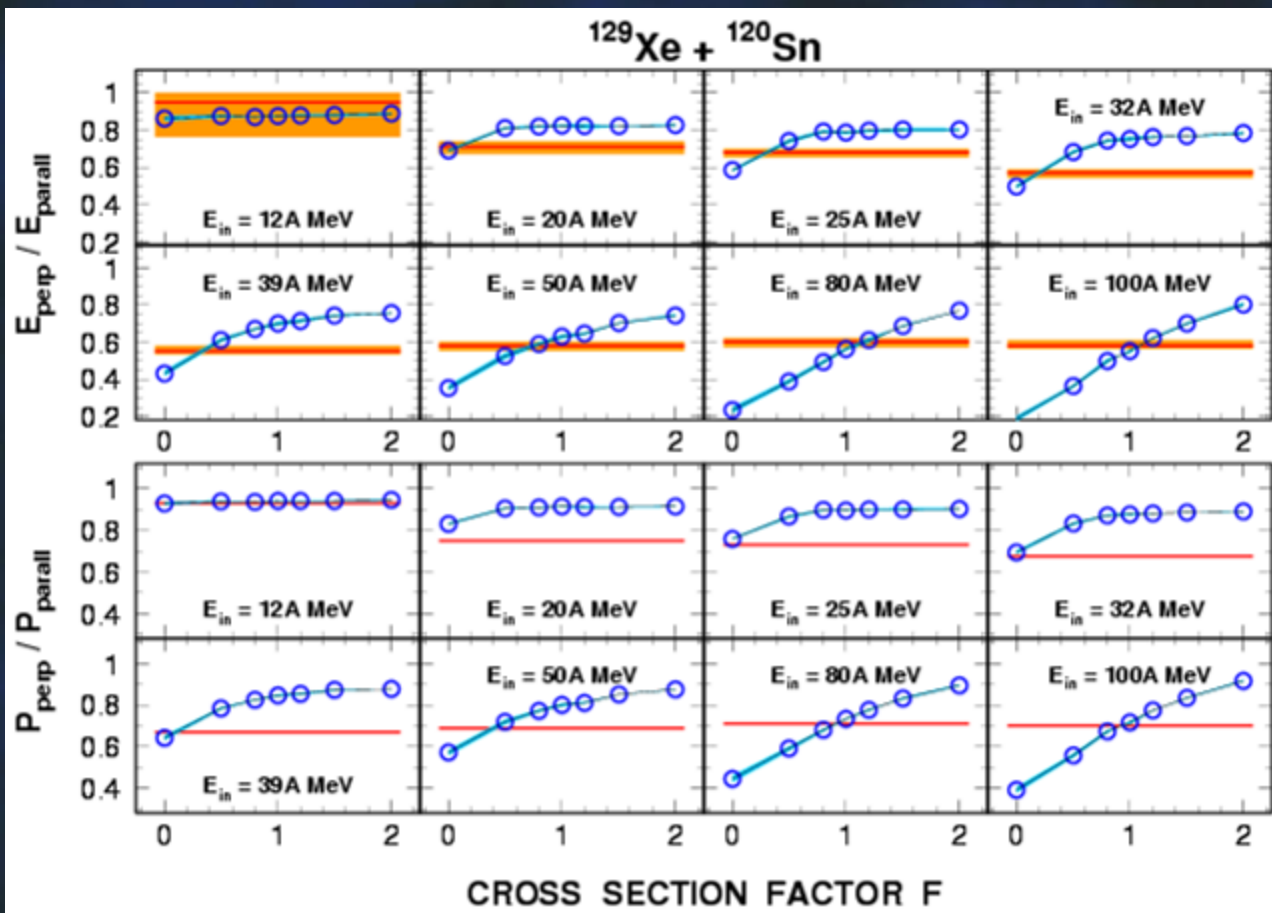


In-medium modifications

$$\sigma_{NN} = (0.8 - 1.2) * \sigma_{Chen}$$



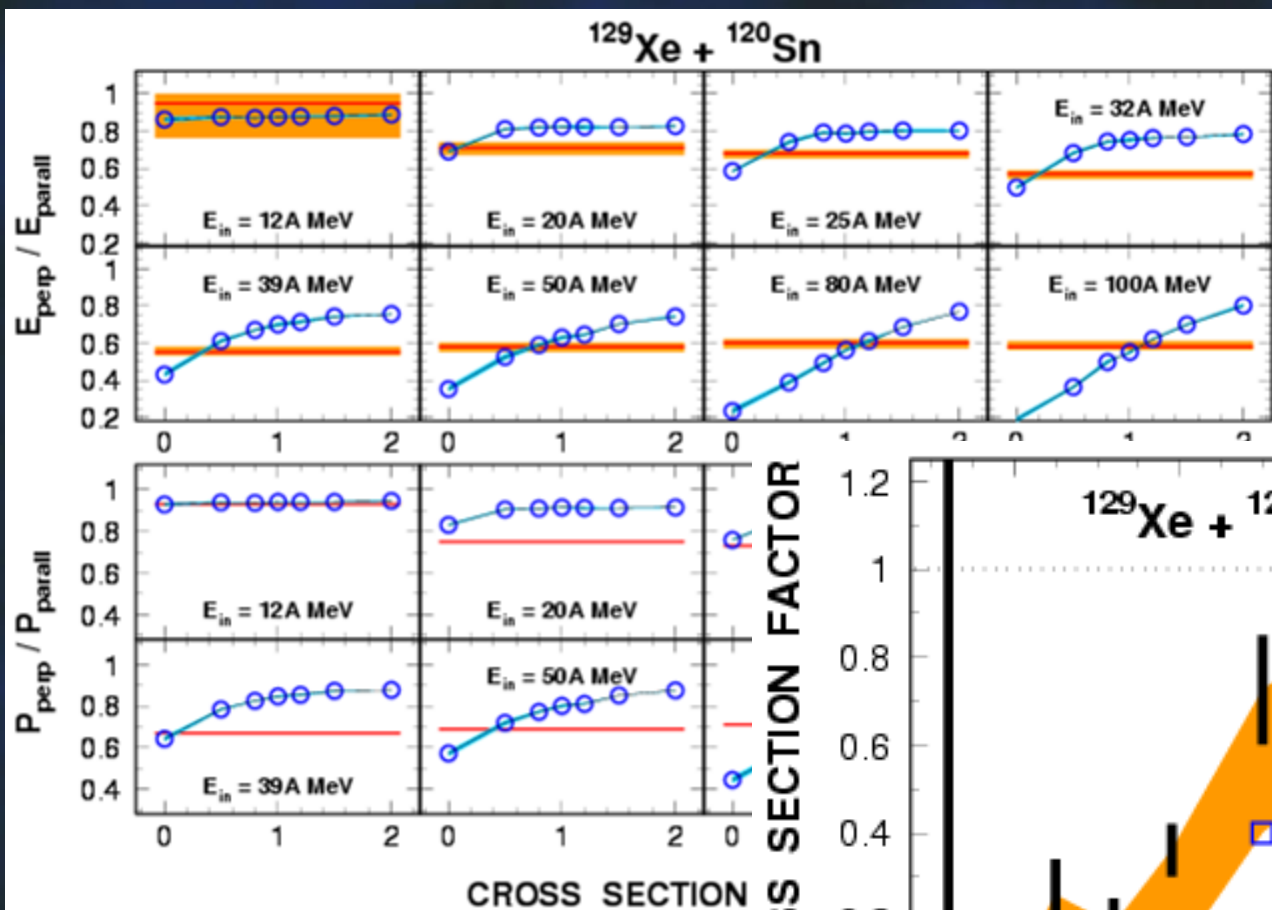
Discrepancy vs. σ_{NN} modification



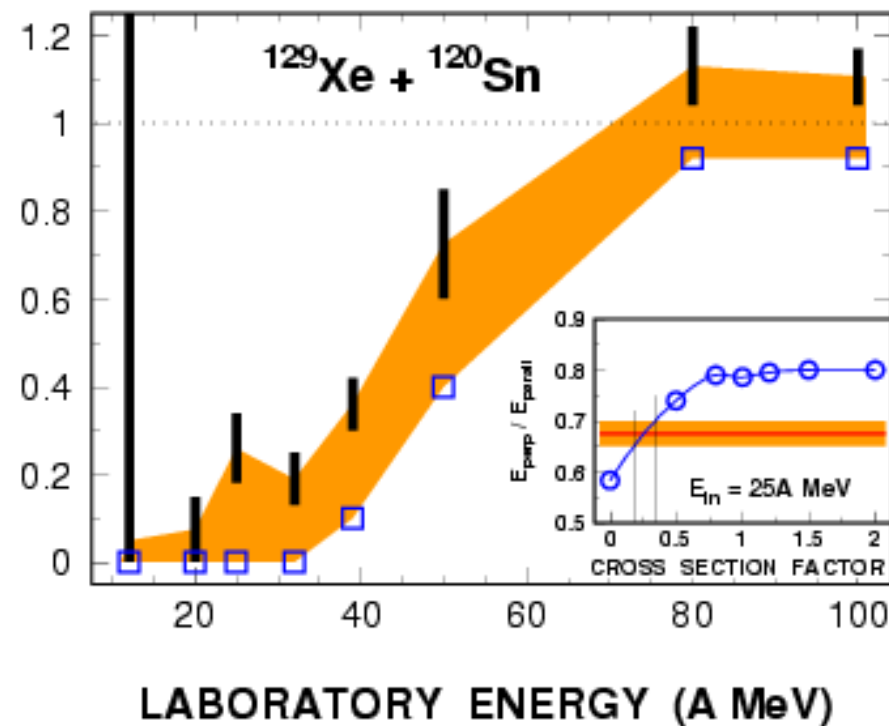
 From INDRA data



Discrepancy vs. σ_{NN} modification



CROSS SECTION FACTOR

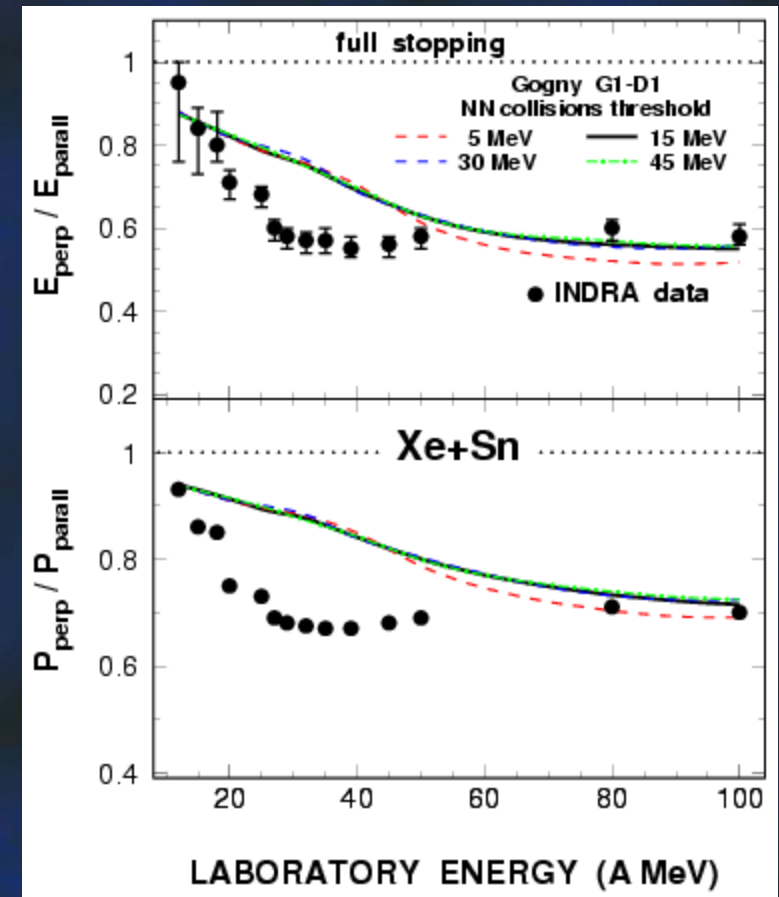


From INDRA data

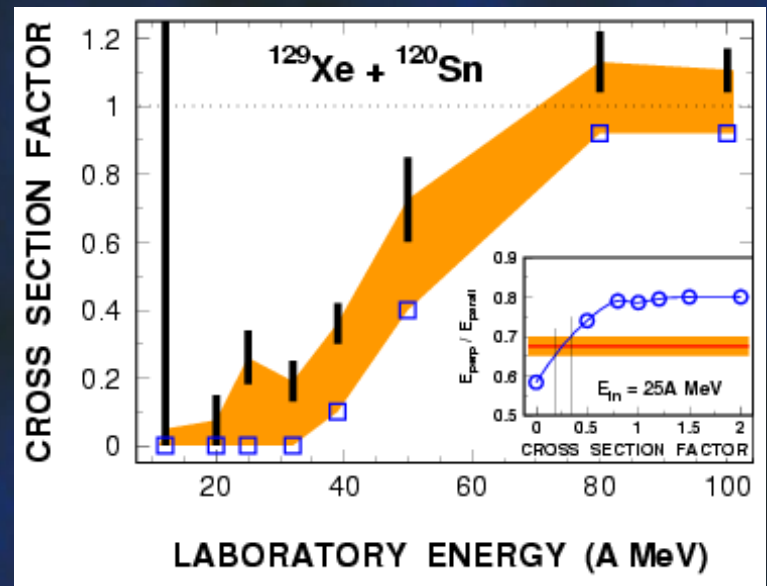
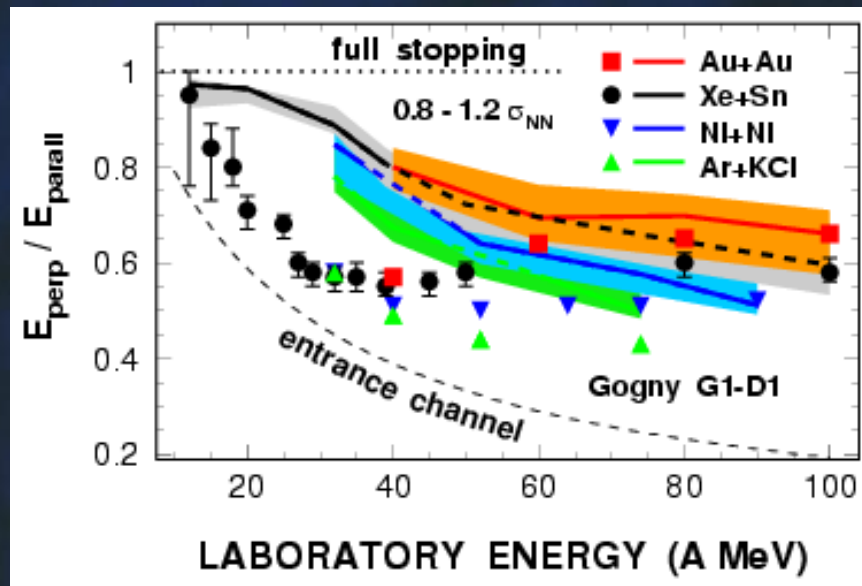


Verification of numerics

- NN collision cut-off energy
- Local potential evaluation box-grid size



Conclusions



- The best EOS non-local Gogny G1-D1
- No (unambiguos) need for in-medium modification of NN cross section
- Strong disagreement data–theory around E_{Fermi}

Pauli blocking

Occupancy tested via:

– **LV**: Local phase space sampling

$$I_{coll} = I_{coll}^{gain} - I_{coll}^{perte} = \frac{g}{4m^2} \cdot \frac{1}{\pi^3 \hbar^3} \int d\mathbf{p}_2 d\mathbf{p}_3 d\mathbf{p}_4 \frac{d\sigma}{d\Omega} \\ \times \delta(\mathbf{p} + \mathbf{p}_2 - \mathbf{p}_3 - \mathbf{p}_4) \delta(p^2 + p_2^2 - p_3^2 - p_4^2)$$

$$\square \cong [(1 - \bar{f})(1 - \bar{f}_2)f_3f_4 - (1 - \bar{f}_3)(1 - \bar{f}_4)f_2f]$$

– **(I)QMD**: Pauli potential

$$U^{\text{Pauli}} = V_p \left(\frac{\hbar}{p_0 q_0} \right)^3 \exp \left(- \frac{(\vec{r}_i - \vec{r}_j)^2}{2q_0^2} - \frac{(\vec{p}_i - \vec{p}_j)^2}{2p_0^2} \right) \delta_{p_i p_j}$$



Summary

- Studied impact of EOS & NN collisions on the stopping observables R_E , R_p
- In partial agreement with the INDRA data: at low E_{in} ($< 20A$ MeV) and above $E_{in} \approx 60A$ MeV
- Largest discrepancy around E_{Fermi}
- Possible cause of the observed discrepancy: Improper accounting for the Pauli principle



Nuclear Stopping at Intermediate Energies - Experiment versus Simulation

Thank you

Zoran Basrak

In collaboration with

Philippe Eudes, Maja Zorić and François Sébille



Laboratory for Nuclear Physics
Division of Experimental Physics
Ruđer Bošković Institute, Zagreb, Croatia

Workshop on Fluctuations and temporal evolution in heavy-ion collisions
May 9 – 10, 2012, Saclay/Paris, France

